



## RESEARCH ARTICLE

10.1002/2015GB005331

## Key Points:

- Decreasing aridity in drylands has a similar effect on soil phosphorus transformations as time
- The Walker and Syers model can be extended to dryland climosequences
- Pedogenic and biogeochemical changes occur at an aridity value of about 0.7

## Supporting Information:

- Supporting Information S1

## Correspondence to:

L. Chen,  
ljchenchina@hotmail.com;  
ljchen@iae.ac.cn

## Citation:

Feng, J., B. L. Turner, X. Lü, Z. Chen, K. Wei, J. Tian, C. Wang, W. Luo, and L. Chen (2016), Phosphorus transformations along a large-scale climosequence in arid and semiarid grasslands of northern China, *Global Biogeochem. Cycles*, 30, 1264–1275, doi:10.1002/2015GB005331.

Received 12 NOV 2015

Accepted 3 AUG 2016

Accepted article online 8 AUG 2016

Published online 1 SEP 2016

## Phosphorus transformations along a large-scale climosequence in arid and semiarid grasslands of northern China

Jiao Feng<sup>1,2</sup>, Benjamin L. Turner<sup>3</sup>, Xiaotao Lü<sup>1</sup>, Zhenhua Chen<sup>1</sup>, Kai Wei<sup>1</sup>, Jihui Tian<sup>1,2</sup>, Chao Wang<sup>1,2</sup>, Wentao Luo<sup>1,2</sup>, and Lijun Chen<sup>1</sup>

<sup>1</sup>Institute of Applied Ecology, Chinese Academy of Sciences, Shenyang, China, <sup>2</sup>College of Resources and Environment, University of Chinese Academy of Sciences, Beijing, China, <sup>3</sup>Smithsonian Tropical Research Institute, Ancon, Panama

**Abstract** The Walker and Syers model of phosphorus (P) transformations during long-term soil development has been verified along many chronosequences but has rarely been examined along climosequences, particularly in arid regions. We hypothesized that decreasing aridity would have similar effects on soil P transformations as time by increasing the rate of pedogenesis. To assess this, we examined P fractions in arid and semiarid grassland soils (0–10 cm) along a 3700 km aridity gradient in northern China (aridity between 0.43 and 0.97, calculated as  $1 - [\text{mean annual precipitation}/\text{potential evapotranspiration}]$ ). Primary mineral P declined as aridity decreased, although it still accounted for about 30% of the total P in the wettest sites. In contrast, the proportions of organic and occluded P increased as aridity decreased. These changes in soil P composition occurred in parallel with marked shifts in soil nutrient stoichiometry, with organic carbon:organic P and nitrogen:organic P ratios increasing with decreasing aridity. These results indicate increasing abundance of P relative to carbon or nitrogen along the climosequence. Overall, our results indicate a broad shift from abiotic to biotic control on P cycling at an aridity value of approximately 0.7 (corresponding to about 250 mm mean annual rainfall). We conclude that the Walker and Syers model can be extended to climosequences in arid and semiarid ecosystems and that the apparent decoupling of nutrient cycles in arid soils is a consequence of their pedogenic immaturity.

### 1. Introduction

Phosphorus (P) is one of the most important elements in biological systems, because it commonly limits terrestrial ecosystem production [Craine *et al.*, 2008; Vitousek *et al.*, 2010] and regulates key ecological processes such as soil organic matter (SOM) accumulation, nitrogen (N) fixation, and carbon (C) stabilization [Walker and Adams, 1958; Mackenzie *et al.*, 2002; Vitousek *et al.*, 2010]. In nature, soil P is derived almost entirely from geochemical weathering of parent material [Lajtha and Schlesinger, 1988], with relatively small inputs from eolian deposition [Okin *et al.*, 2004; Selmants and Hart, 2010]. Plants and microbes incorporate P into biomass and return it to the soil in organic forms, which can then be recycled by phosphatase enzymes to release inorganic phosphate for biological uptake [Walker and Syers, 1976; Cross and Schlesinger, 1995; Turner *et al.*, 2007]. The P cycle is therefore regulated by both geochemical and biological processes [Cross and Schlesinger, 2001; Delgado-Baquerizo *et al.*, 2013]. Identifying and quantifying the transformations and pools of soil P can provide insight into the abiotic and biotic controls on the availability of this essential nutrient [Cross and Schlesinger, 2001; Delgado-Baquerizo *et al.*, 2013].

The amount and chemical composition of soil P are related to pedogenesis [Walker, 1965; Walker and Syers, 1976; Lajtha and Schlesinger, 1988; Turner *et al.*, 2007; Yang and Post, 2011]. Based on four soil chronosequences developed in contrasting climates and ecosystems in New Zealand, Walker and Syers [1976] proposed a general model to predict the dynamics of P during long-term pedogenesis. Phosphorus released from primary minerals by weathering can become sorbed to soil particles, lost from the soil profile in leachate, or assimilated by biomass and enter the organic P ( $P_o$ ) pool. Over longer timescales, P can become associated with secondary minerals such as aluminum (Al) and iron (Fe) oxides and transformed into stable forms known collectively as occluded P. In old soils on stable land surfaces, a “terminal steady state” is reached, whereby primary mineral P is exhausted, the total P concentration is low, P input from dust deposition is of similar magnitude to P export in runoff, and the remaining soil P is predominantly in organic and occluded inorganic forms [Walker and Syers, 1976].

Compared to soils in more humid regions, arid soils typically contain little SOM, and carbonate minerals are the predominant reservoir of P [Lajtha and Schlesinger, 1988; Cross and Schlesinger, 1995]. This is due mainly to reduced water inputs in arid environments, which limits leaching and allows calcium (Ca) minerals to accumulate [Lajtha and Schlesinger, 1988; Ippolito et al., 2010]. In addition, little P is incorporated into biomass because of water limitation, leading to a small  $P_o$  pool in arid soils [Lajtha and Schlesinger, 1988; Delgado-Baquerizo et al., 2013]. Weathering of primary minerals is thus more important than biological mineralization of  $P_o$  in supplying P to plants in arid soils [Delgado-Baquerizo et al., 2013]. In humid soils, however, a greater proportion of the P occurs in organic compounds or bound to secondary Al and Fe oxides, which can reduce P availability to plants and microbes [Walker and Syers, 1976; Cross and Schlesinger, 1995; McGroddy et al., 2008]. Biological mineralization of  $P_o$  is therefore essential to maintain the bioavailable P pool in humid sites [Walker and Syers, 1976; Crews et al., 1995; Izquierdo et al., 2013]. These differences could cause the biogeochemical transformations and availability of P to differ fundamentally between arid and humid soils [Cross and Schlesinger, 1995; Ippolito et al., 2010].

Walker and Syers [1976] suggested that compared to humid sites, it would take longer for soil P transformations to occur in arid sites with low leaching intensity. They were therefore careful to predict that their model would apply only to soils formed under humid ecosystems on stable land surfaces [Walker and Syers, 1976; Turner and Condon, 2013]. The Walker and Syers model has since been validated along a number of chronosequences in humid ecosystems [Tiessen et al., 1984; Crews et al., 1995; Vitousek and Farrington, 1997; Richardson et al., 2004; Izquierdo et al., 2013], yet only a few studies have been conducted in more arid ecosystems [Lajtha and Schlesinger, 1988; Selmants and Hart, 2010; Turner and Laliberté, 2015]. Lajtha and Schlesinger [1988] observed little transformation of P from Ca-bound forms to Fe- and Al-bound forms even in the oldest soils of an arid chronosequence (25,660 years B.P.), which they attributed to the low weathering intensity. However, Selmants and Hart [2010] observed decreasing primary mineral P and increasing  $P_o$  across a 3 million year volcanic chronosequence in northern Arizona, USA, demonstrating that the Walker and Syers model can also apply to soils under (modern) arid climates. These results highlight the uncertainty in applying the Walker and Syers model to ecosystem development under arid and semiarid climates.

Walker and Syers [1976] proposed that soil development sequences consisted of soils arranged in order of enhanced development (weathering) brought about by greater age, greater precipitation, or decreasing slope. They suggested that pedogenesis was determined by the quantity of water leached through the soil profile, irrespective of whether this was driven by increasing soil age at constant precipitation, or by increasing precipitation in soils of the same age [Walker and Syers, 1976]. They observed substantial transformations of soil P with pedogenesis across several soil sequences in New Zealand, including chronosequences, toposequences, and hydrosequences [Walker and Syers, 1976]. Although particular emphasis has been placed subsequently on P transformations along soil chronosequences [Crews et al., 1995; Turner et al., 2007; Selmants and Hart, 2010; Turner and Condon, 2013; Chen et al., 2015; Turner and Laliberté, 2015], relatively few studies have examined climosequences [Ippolito et al., 2010; Emadi et al., 2012] or toposequences [Roberts et al., 1985; Agbenin and Tiessen, 1995].

In drier ecosystems, water availability is the critical determinant of the rate of weathering and pedogenesis and often drives substantial changes in soil physical and chemical characteristics [Ippolito et al., 2010; Khormali and Kehl, 2011; Quénard et al., 2011]. Delgado-Baquerizo et al. [2013] argued that C, N, and P cycles became decoupled with increasing aridity (manifested as decreases in soil C:P and N:P ratios), which they attributed to differences in the response of P to increasing aridity compared to the responses of C and N. Wardle [2013] commented that these decoupled nutrient cycles with increasing aridity operated in the opposite direction of ecosystem development. It could be argued therefore that climate might have similar effects on soil genesis and P cycling as time, with wetter soils equating to older soils in terms of greater P loss, wider C:P ratios, and stronger P limitation of biological processes [Walker and Syers, 1976; Crews et al., 1995; Selmants and Hart, 2010; Chen et al., 2015; Turner and Laliberté, 2015]. Consistent with this, Ippolito et al. [2010] observed a distinct decrease in Ca-bound P and an increase in occluded P with increasing precipitation across the central Great Plains in the USA, indicating the strong effect of precipitation on pedogenesis and P transformations in drier ecosystems.

We collected soil from 52 sites along a 3700 km grassland transect in northern China. The transect is considered to represent a climate gradient and has been used to study how climate influences aboveground and

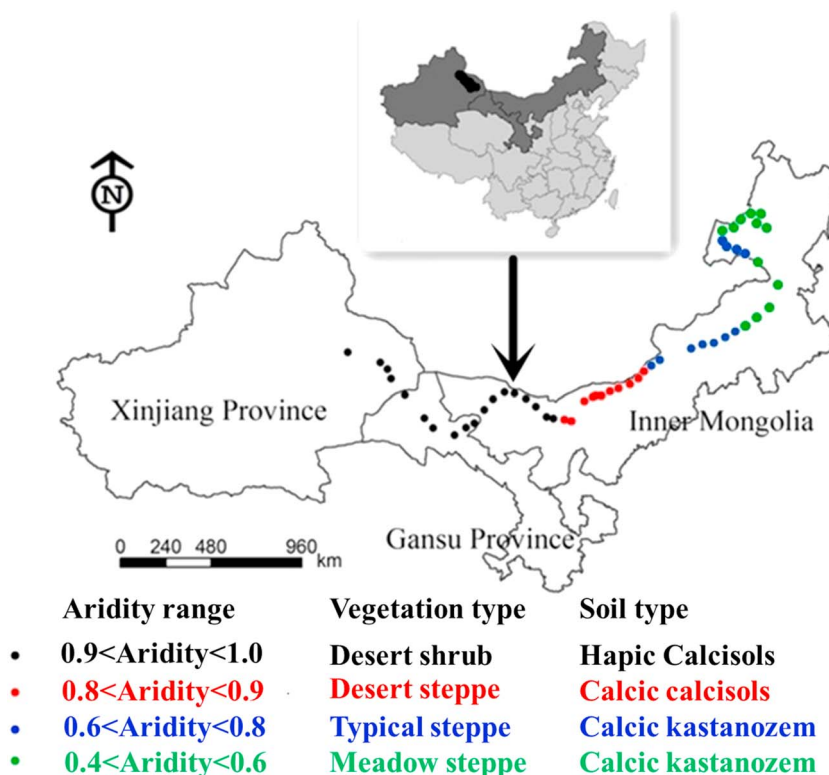


**Figure 1.** Geographic distribution of sample sites. Fifty-two sites were selected along a 3700 km aridity gradient in northern China. Aridity ranged from 0.97 in the west to 0.43 in the east.

belowground ecological processes and predict their responses to global climate change [Zhou *et al.*, 2002; Wang *et al.*, 2014; Luo *et al.*, 2015]. The transect provides an opportunity to investigate large-scale climate-driven P transformations in drylands. Increased aridity is predicted in global drylands [Gao and Giorgi, 2008; Feng and Fu, 2013], so patterns of P chemistry along the climosequence can inform our understanding and ultimately our ability to predict how biogeochemical P cycling will be affected by climate change.

We aimed to (1) identify and quantify soil P fractions in arid and semiarid ecosystems across the climosequence, (2) assess the relative importance of abiotic and biotic controls on P availability in these drylands, and (3) test whether soil P transformations along the climosequence are consistent with the predictions of the Walker and Syers [1976] model and are comparable to the patterns of soil P transformations along humid soil chronosequences.

## 2. Materials and Methods

### 2.1. Study Sites

The study was conducted along a 3700 km west-to-east transect across Xinjiang, Gansu province, and Inner Mongolia, primarily on the Inner Mongolian Plateau (Figure 1). Elevation declines from about 1200 m in the west to approximately 600 m in the east. However, the topography is muted, with tablelands and gently rolling hills [Luo *et al.*, 2016], allowing us to eliminate this soil-forming factor as a major driver of pedogenesis along the climate gradient. The mean annual precipitation (MAP) increased from 34 mm in the west to 436 mm in the east, with 77%–98% (mean 88%) of the precipitation occurring between June and September. The mean annual temperature (MAT) varied from about 10°C in the western sites to –3°C in the eastern sites. The monthly mean temperature was below 0°C in winter and early spring (between November and March) at all sites along the transect. The highest temperature occurred between June and August, with monthly mean temperature between 25°C and 15°C (mean 20°C) from west to east along the transect. Annual potential evapotranspiration (PET) declined from about 1200 mm in the west to about 710 mm in the east. MAT was negatively correlated with MAP along the transect ( $R^2 = 0.889$ ,  $P < 0.001$ , Figure S1 in the supporting information). By including both MAP and MAT, the aridity measure provides an

integrated index of variation of climate (equation (1)) [Arora, 2002], with aridity correlating negatively with MAP ( $R^2 = 0.992$ ,  $P < 0.001$ ) and positively with MAT ( $R^2 = 0.898$ ,  $P < 0.001$ , Figure S1).

$$\text{Aridity} = 1 - \frac{\text{MAP}}{\text{PET}} \quad (1)$$

In the western sites, high temperature (high PET) coupled with low precipitation results in an extremely arid climate. In the eastern sites, low temperature (low PET) and high precipitation together alleviate the aridity. From west to east, aridity declines from 0.97 to 0.43 along the transect, indicating decreasing aridity and increasing humidity. Following this aridity gradient from dry (west; low precipitation, high temperature, and PET) to wet (east; high precipitation, low temperature, and PET), ecosystem type shifts gradually from arid grassland to semiarid grassland, and the dominant vegetation types are desert shrub, desert steppe, and typical steppe followed by meadow steppe (Figure 1).

Soils along the transect began forming during the Holocene [Liangwu and Angjiang, 2001; Feng *et al.*, 2006] and are therefore relatively weakly developed, with high concentrations of calcareous sediments close to the soil surface [Irwin-Williams and Haynes, 1970; Feng *et al.*, 2006]. The soils are formed primarily from loess deposits, although some have formed in diluvial and alluvial deposits, and desert soils in the western sites can also receive eolian sands. Soils varied with decreasing aridity from Haplic Calcisols in the drier sites, to Calcic Cambisols at intermediate rainfall, and then Calcic Kastanozems at the wetter sites (Figure 1). Haplic Calcisols are characterized by calcium carbonate accumulation at the soil surface and lack a calcic horizon (Bk) and are therefore in an initial stage of soil formation. Calcic Cambisols have minimal B horizon development and are considered to be in an intermediate stage of development [Food and Agriculture Organization (FAO), 1993]. Calcic Kastanozems are relatively mature soils with well-developed soil profiles, with secondary (pedogenic) carbonate accumulation at depth (i.e., with calcic horizons) [FAO, 1993]. Thus, the CaO content of surface soils along the transect declines from about 7% in Haplic Calcisols, to 3% in Calcic Cambisols, and then 1% in Calcic Kastanozems [Lei *et al.*, 1990; Shi *et al.*, 1990] but has accumulated in subsurface horizons in Calcic Cambisols (20–50 cm) and Calcic Kastanozems (>40 cm deep) [Lei *et al.*, 1990; Shi *et al.*, 1990].

All surface soils across the transect are sands or sandy loams, with >60% sand and a strong acid reaction (Figure S2) [Wang *et al.*, 2014, 2016]. The elemental composition of surface soil is similar in all three soil classes, with composition after ignition dominated by SiO<sub>2</sub> (70–76%), with smaller amounts of Al<sub>2</sub>O<sub>3</sub> (11–12%) and Fe<sub>2</sub>O<sub>3</sub> (3–4%) [Lei *et al.*, 1990; Shi *et al.*, 1990]. This limited range in elemental composition suggests that the parent loess is relatively homogenous across the transect.

Fifty-two sites were sampled at 50–100 km intervals along the climosequence during July–August 2012. The geographical location and elevation of each site were recorded by Global Positioning Satellite device (eTrex Venture, Garmin, USA). At each site, five 1 m × 1 m subplots were selected within a 50 m × 50 m plot. In each subplot, all grasses were harvested for calculation of aboveground primary production (ANPP). In a 5 m × 5 m subplot with shrubby vegetation, one fourth of annual branches were clipped to measure ANPP (expressed as per square meter). Three soil samples were collected using a 100 cm<sup>3</sup> cylinder (5 cm height × 5 cm diameter) to determine soil bulk density, and then 20 soil cores (0–10 cm depth, 2.5 cm diameter) were collected at random and homogenized. Stones and visible roots were removed in situ; soils were sieved (<2 mm) and stored in plastic bags. A subsample was stored at 4°C in the field and then frozen at –20°C upon return to the laboratory for biological analyses. A second subsample was immediately air-dried after sampling for the determination of abiotic properties. More detailed descriptions of the study region and sampling protocol can be found in Wang *et al.* [2014] and Luo *et al.* [2015].

## 2.2. Determination of Soil Total, Inorganic, and Organic Phosphorus

Total P (P<sub>t</sub>) was determined by igniting soil in a muffle furnace at 550°C for 1 h [Aspila *et al.*, 1976]. A second subsample of unignited soil was used to determine the total inorganic P (P<sub>i</sub>) concentration. Both ignited and unignited samples were shaken in 1 M H<sub>2</sub>SO<sub>4</sub> for 16 h at 25°C in a 1:30 soil to solution ratio and filtered through a 30–50 μm cellulose-nitrate membrane filter (ASTME832-81). Phosphate was determined at 880 nm by molybdate colorimetry on a spectrophotometer (Cary 500, Varian Company, USA). Soil P<sub>o</sub> was estimated as the difference in P in ignited and unignited samples. This procedure can underestimate P<sub>t</sub> in strongly weathered soils but is generally appropriate for weakly and moderately weathered soils such as those along our climosequence [Hance and Anderson, 1962; Williams *et al.*, 1970].

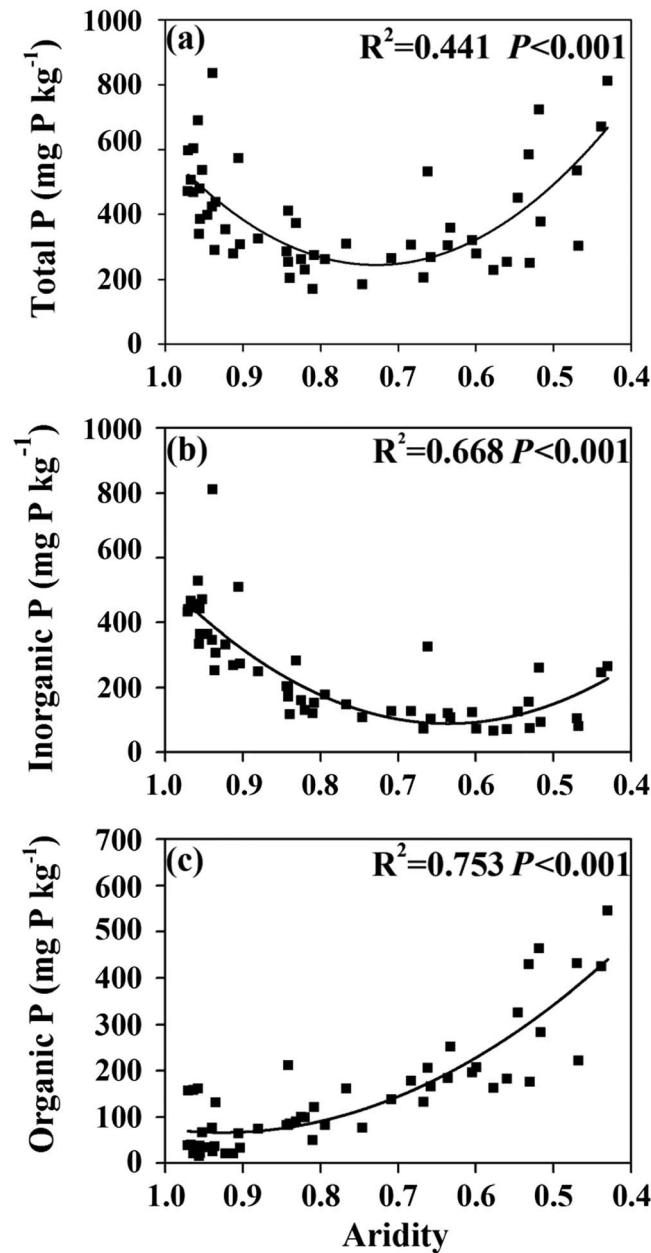


**Figure 2.** Soil total phosphorus, inorganic phosphorus, and organic phosphorus concentrations.

$P_t$  in the extracts, with  $P_o$  calculated as the difference between  $P_t$  and  $P_i$ . All extracts were determined by molybdate colorimetry at 880 nm on a spectrophotometer (Cary 500, Varian Company, USA). Available- $P_i$  was the sum of resin-P and  $\text{NaHCO}_3$ - $P_i$ ; total  $P_i$  was the sum of resin-P,  $\text{NaHCO}_3$ - $P_i$ ,  $\text{NaOH}$ - $P_i$ , and  $\text{HCl}$ - $P_i$ ; total extracted  $P_o$  was the sum of  $\text{NaHCO}_3$ - $P_o$ ,  $\text{NaOH}$ - $P_o$ , and  $\text{HCl}$ - $P_o$ ;  $P_t$  was the sum of  $P_i$  and  $P_o$ . For comparison with the Walker and Syers [1976] model, the sequential P fractions were grouped into  $P_{Ca}$  ( $\text{HCl}$ - $P_i$ ), occluded P (residual P), nonoccluded P (sum of resin-P,  $\text{NaHCO}_3$ - $P_i$ , and  $\text{NaOH}$ - $P_i$ ), and  $P_o$  (sum of  $\text{NaHCO}_3$ - $P_o$ ,  $\text{NaOH}$ - $P_o$ , and  $\text{HCl}$ - $P_o$ ).

**2.4. Climate Data**

Mean annual temperature, MAP and PET for each sampling site was extracted from the WorldClim data set using ArcGIS version 9.3 (Esri, Redlands, CA).

**2.3. Sequential Phosphorus Fractionation**

Phosphorus fractions were extracted by a modified sequential Hedley fractionation scheme [Tiessen and Moir, 1993]. First, resin-P was determined by shaking 1.000 g soil (dry weight) with 30 mL of deionized water and a clean anion-exchange resin strip (2.5 × 1 cm, 551642S, BDH-Prolabo, VWR International, Lutterworth, UK) in a 50 mL plastic centrifuge tube for 16 h at 25°C in an overhead shaker. Phosphorus retained on the resin strip was eluted by shaking the resin strip with 10 mL 0.25 M  $\text{H}_2\text{SO}_4$  for 1 h. The soil sample was centrifuged at 8180 × g for 10 min, the supernatant decanted, and the remaining soil was shaken with 30 ml of 0.5 M  $\text{NaHCO}_3$  (pH=8.5) for 16 h at 25°C ( $\text{NaHCO}_3$ -P). Using the same procedure, the remaining sample was then sequentially extracted with 0.1 M  $\text{NaOH}$  and 1 M  $\text{HCl}$  to extract  $\text{NaOH}$ -P and  $\text{HCl}$ -P, respectively. The hot  $\text{HCl}$  extraction step, introduced by Tiessen and Moir [1993] for strongly weathered tropical soils, was not included because the calcic soils in this study do not contain significant proportions of recalcitrant P associated with secondary minerals. Finally, the residue was ignited in a muffle furnace at 550°C for 1 h to determine residual P. Aliquots of the  $\text{NaHCO}_3$ ,  $\text{NaOH}$ , and  $\text{HCl}$  extracts were digested with  $\text{K}_2\text{S}_2\text{O}_8$ - $\text{H}_2\text{SO}_4$  to determine

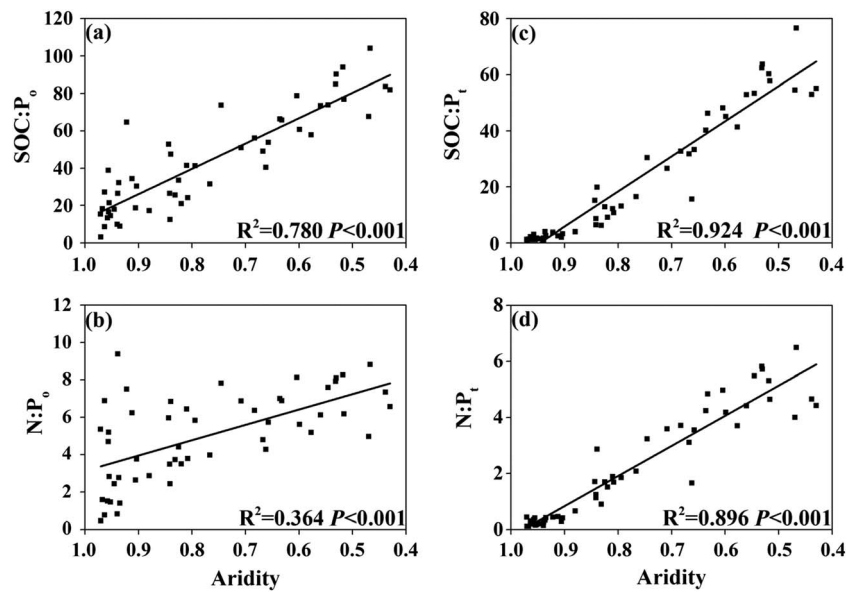


**Figure 3.** Soil elemental ratios (soil organic carbon, SOC; total nitrogen, N; total phosphorus, P<sub>t</sub> and organic phosphorus, P<sub>o</sub>) across the aridity gradient.

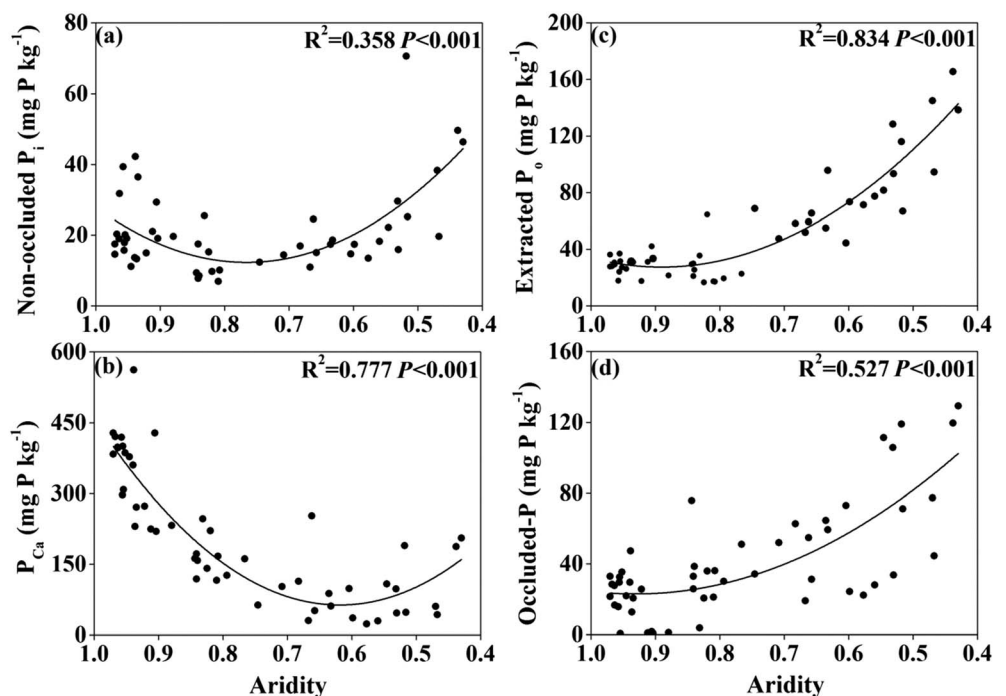


**Figure 4.** Changes in nonoccluded P (sum of resin-P, NaHCO<sub>3</sub>-P<sub>i</sub>, and NaOH-P<sub>i</sub>, mg P kg<sup>-1</sup>), P<sub>Ca</sub> (primary mineral P, i.e., HCl-P<sub>i</sub>, mg P kg<sup>-1</sup>), extracted P<sub>o</sub> (sum of NaHCO<sub>3</sub>-P<sub>o</sub>, NaOH-P<sub>o</sub>, and HCl-P<sub>o</sub>, mg P kg<sup>-1</sup>), and occluded P (residual P, mg P kg<sup>-1</sup>).

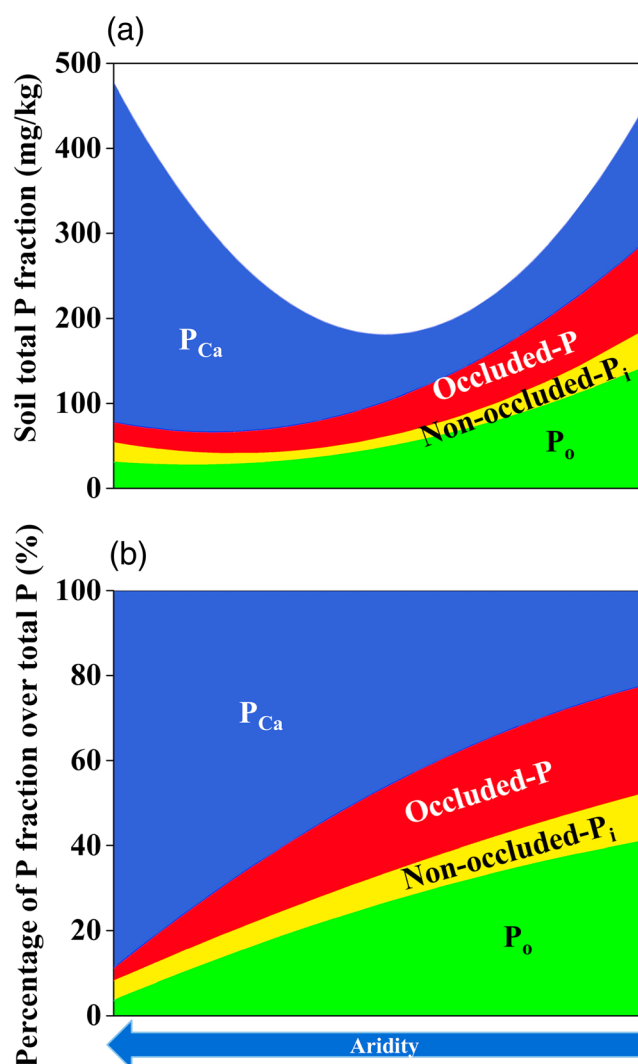


**Figure 5.** Panels of P fractions along the climosequence in arid and semiarid ecosystems in northern China: the comparison to Walker and Syers diagram. (a) The amount of absolute P fraction and (b) the percentage of P fraction in total P (%). Curves were obtained by polynomial fitting between aridity and P fractions based on 52 sample sites.  $P_{Ca}$  represents calcium phosphates in primary minerals extracted by HCl- $P_i$ . Occluded P represents residual P. Nonoccluded  $P_i$  is the sum of resin-P,  $\text{NaHCO}_3$ - $P_i$ , and NaOH- $P_i$ .  $P_o$  is the sum of  $\text{NaHCO}_3$ - $P_o$ , NaOH- $P_o$ , and HCl- $P_o$ .

Nonoccluded  $P_i$  (sum of resin-P,  $\text{NaHCO}_3$ - $P_i$ , and NaOH- $P_i$ ) accounted for < 14% of  $P_t$  (average 7%, 6 to 70 mg P kg<sup>-1</sup>) (Figures 4a and S4). This pool decreased initially and then increased across the aridity gradient from dry to wet, with the minimum value at aridity of approximately 0.70 (Figure 4a). The  $P_{Ca}$  (HCl- $P_i$ ) varied between 23 and 562 mg P kg<sup>-1</sup> and accounted for the largest proportion of  $P_t$  (18–87%, mean 60%). The  $P_{Ca}$  concentration generally declined across the aridity gradient from dry to wet (Figure 4b). Soil-extracted  $P_o$  (the sum of  $\text{NaHCO}_3$ - $P_o$ , NaOH- $P_o$ , and HCl- $P_o$ ) varied between 17 and 165 mg P kg<sup>-1</sup> (4–55% of  $P_t$ , mean 19%) and increased progressively across the aridity gradient from dry to wet, with a slight increase in drier sites but a marked accumulation in wetter sites (Figure 4c). The concentration of NaOH- $P_o$  ranged from 2 to 130 mg P kg<sup>-1</sup> (33 mg P kg<sup>-1</sup> on average) and constituted on average 73% of total extractable  $P_o$ .  $\text{NaHCO}_3$ - $P_o$  (0–20 mg P kg<sup>-1</sup>) and HCl- $P_o$  (0–45 mg P kg<sup>-1</sup>) accounted for 12% and 15% of total extractable  $P_o$  on average, respectively (Figure S4). Occluded P (residual P, the most tightly bound P pool) accounted

## 2.5. Statistical Analysis

Pearson correlation analysis was carried out to quantify relationships between key soil chemical properties and concentrations of P fractions (SPSS 16.0, Benelux BV, Gorinchem, Netherlands). Regression analyses were used to fit linear and polynomial data using Origin 9.0 software (OriginLab Corp., Northampton, MA, USA). Ordinary least squares polynomial fitting was used to examine the relationships of aridity with soil  $P_t$ ,  $P_o$ , and  $P_i$ , and with soil P fractions as well. Ordinary least squares linear fitting was used to analyze the relationships between aridity and elemental ratios of soil C, N, and P.

## 3. Results

### 3.1. Soil Phosphorus Fractions and Soil Elemental Ratios Across the Aridity Gradient

Soil  $P_t$  decreased from about 500 mg P kg<sup>-1</sup> to about 300 mg P kg<sup>-1</sup> in drier sites (aridity > 0.70), followed by an increase to around 600 mg P kg<sup>-1</sup> in wetter sites (aridity < 0.70; Figure 2a). Soil  $P_i$  declined, while  $P_o$  increased continuously along the climosequence from dry to wet (Figures 2b and 2c). Soil  $P_o$  was correlated negatively with MAT ( $R^2 = 0.659$ ,  $P < 0.001$ , Figure S3), but positively with MAP ( $R^2 = 0.805$ ,  $P < 0.001$ , Figure S3). Soil organic C (SOC): $P_o$ , N: $P_o$ , SOC: $P_t$ , and N: $P_t$  ratios were all correlated negatively with aridity (Figure 3).

**Table 1.** Pearson Correlation Coefficients Among Key Soil Chemical Properties and Concentrations ( $\text{mg P kg}^{-1}$ ) of Phosphorus Fractions in Soils Along the Grassland Transect in Northern China<sup>a</sup>

	$P_t$	$P_i$	Extracted $P_o$	Available- $P_i$	NaOH- $P_i$	HCl- $P_i$	$\text{NaHCO}_3$ - $P_o$	NaOH- $P_o$	HCl- $P_o$	Residual P
pH	ns	0.535*	-0.834**	ns	-0.787**	0.575**	ns	-0.861**	ns	-0.631**
$\text{Ca}^{2+}$	0.537**	0.641**	-0.348*	ns	-0.337*	0.651**	ns	-0.340*	ns	ns
$\text{Fe}^{2+}$	ns	ns	0.770**	0.487**	0.855**	ns	ns	0.823**	ns	0.663**
$\text{Mn}^{2+}$	ns	ns	0.822**	0.488**	0.905**	-0.295*	ns	0.847**	ns	0.750**

<sup>a</sup> Available- $P_i$ : sum of resin-P and  $\text{NaHCO}_3$ - $P_i$ ;  $P_i$ : sum of available- $P_i$ , NaOH- $P_i$ , and HCl- $P_i$ ; Extracted  $P_o$ : sum of  $\text{NaHCO}_3$ - $P_o$ , NaOH- $P_o$ , and HCl- $P_o$ ;  $P_t$ : sum of  $P_i$ ,  $P_o$ , and residual P.

\* $p < 0.05$ .

\*\* $p < 0.01$  ( $n = 52$ ); ns, not significant.

for 14% of  $P_t$  on average (0 to  $129 \text{ mg P kg}^{-1}$ , 0 to 34% of  $P_i$ ), and progressively increased across the aridity gradient from dry to wet (Figure 4d).

Changes in soil P pools along the climosequence are plotted in the same manner as the original Walker and Syers [1976] diagram of P transformations with time (Figure 5). The concentration and proportion of  $P_{Ca}$  declined, while that of occluded P and extracted  $P_o$  increased with soil development (i.e., as a function of declining aridity) (Figure 5). Soil  $P_t$ , calculated by the sum of all fractions ( $112\text{--}684 \text{ mg P kg}^{-1}$ ), did not decline significantly across the climosequence. There was an initial decrease in  $P_t$  in drier sites followed by an almost equal increase in wetter sites (Figure 5a).

### 3.2. Relationship Between Soil Total Phosphorus Determined by Different Methods

Soil  $P_t$  determined by sequential extraction (i.e., the sum of extracted  $P_i$ ,  $P_o$ , and residual P, Figure 5) was correlated strongly with an independent measure of  $P_t$  determined by the ignition procedure ( $R^2 = 0.775$ ,  $p < 0.01$ ,  $n = 52$ ). Generally,  $P_t$  by sequential extraction was approximately  $18\% \pm 8\%$  less than  $P_t$  determined by ignition. This is likely due to systematic errors in the sequential fractionation method [Tiessen and Moir, 1993]. Overall, the values of  $P_t$  by different methods were comparable in these arid and semiarid grassland ecosystems.

### 3.3. Relationships Between Soil Chemical Properties and Phosphorus Fractions

Extracted  $P_i$  and the dominant  $P_i$  fraction (HCl- $P_i$ ) were correlated positively with soil pH and soil exchangeable Ca, with Pearson product-moment correlation coefficients ( $r$ ) between 0.535 and 0.651 ( $p < 0.05$ , Table 1). Conversely, total extracted  $P_o$ , NaOH- $P_i$ , and NaOH- $P_o$  were correlated negatively with soil pH ( $r$  from  $-0.631$  to  $-0.861$ ,  $p < 0.01$ ) and soil exchangeable Ca ( $r$  from  $-0.337$  to  $-0.348$ ,  $p < 0.05$ ). Soil available- $P_i$ , NaOH- $P_i$ , NaOH- $P_o$ , and residual P were correlated positively with both soil exchangeable Fe ( $r$  from 0.487 to 0.855,  $p < 0.01$ ) and Mn ( $r$  from 0.488 to 0.905,  $p < 0.01$ ).

## 4. Discussion

Changes in the concentrations and proportions of  $P_{Ca}$ ,  $P_o$ , and occluded P along our climosequence are consistent with expectations of changes in soil P fractions during pedogenesis [Walker and Syers, 1976]. Based on a series of soil sequences in New Zealand, Walker and Syers suggested that pedogenesis depended predominantly on the volume of water leached through soil, irrespective of whether this occurred through increasing soil age at constant water availability or by increasing water availability in soils of the same age [Walker and Syers, 1976]. The strong redistribution of P from primary minerals to  $P_o$  and occluded P pools along our climosequence supports the application of the Walker and Syers [1976] model to arid and semiarid ecosystems, not just across chronosequences but also along climosequences.

The concentration of  $P_{Ca}$  generally declined with decreasing aridity, except for three relatively higher values in the wettest sites, which may be outliers due to their relatively low sand contents (Figure S2). The general decline of the  $P_{Ca}$  pool with decreasing aridity agrees with the prediction of the Walker and Syers [1976] model and the findings of many previous studies that examined the primary stages of soil genesis [e.g., Syers and Walker, 1969a; Ippolito et al., 2010; Selmants and Hart, 2010]. The decline of  $P_{Ca}$  corresponds with a marked decline in soil exchangeable Ca in our climosequence [Luo, 2015], suggesting enhanced leaching



of  $P_{Ca}$  along with weatherable cations. This is consistent with results from previous studies along chronosequences in humid and Mediterranean ecosystems, in which  $P_{Ca}$  declined rapidly during the initial stages of soil development [Syers and Walker, 1969a; Walker and Syers, 1976; Richardson et al., 2004; Turner and Laliberté, 2015]. However,  $P_{Ca}$  still constituted about 30% of the  $P_t$  in the wettest soils along our climosequence, in contrast to similar-aged soils in humid ecosystems, such as tropical forests in New Zealand and Hawaii, where  $P_{Ca}$  is exhausted after approximately 10,000 years of pedogenesis [Walker and Syers, 1976; Crews et al., 1995]. This reflects the fact that the wettest sites in our study receive only about 400 mm of annual precipitation, which has been insufficient to completely deplete the soil of  $P_{Ca}$ . The pattern of  $P_{Ca}$  along the climosequence supports the prediction of Walker and Syers [1976] that P transformation are slower in arid sites with low leaching intensity and suggests that soils along our climosequence are still pedogenically immature.

Occluded P and  $P_o$  that is mostly associated with Al and Fe oxides (NaOH- $P_o$ , the main  $P_o$  fraction, Figure S2) gradually increased along the climosequence, both in absolute terms and as a fraction of  $P_t$  (Figures 4c, 4d, and 5), as has been widely demonstrated by chronosequence studies of the early stages of soil development [Syers and Walker, 1969b; Walker and Syers, 1976; Lajtha and Schlesinger, 1988; Ippolito et al., 2010]. Along our climosequence, greater  $P_o$  concentrations are associated with increasing biomass production (i.e., ANPP and microbial biomass carbon (MBC)) [Wang et al., 2014] and greater associated P inputs as organic residues along the climosequence [Cross and Schlesinger, 1995, 2001; Ippolito et al., 2010]. Moreover, we observed significant positive correlations between extracted  $P_o$  and exchangeable Fe and Mn (Table 1), suggesting that the high specific surface areas of these metal oxides [Luo, 2015] sorb and stabilize  $P_o$  in the soil [Celi et al., 1999; Turner et al., 2002]. Further,  $P_o$  and MAT were negatively correlated along the transect (Figure S3), suggesting that low temperatures might also contribute to the accumulation of  $P_o$  in wetter sites through reduced microbial activity [Post et al., 1985; Zheng et al., 2009; Wang et al., 2014]. In weakly and moderately weathered soils, occluded P is mostly recalcitrant  $P_o$  [Williams et al., 1967; Walker and Syers, 1976], suggesting that the increase in occluded P with pedogenesis might be related to the increase in total  $P_o$  with decreasing aridity.

A notable difference between our results and the Walker and Syers [1976] model is the behavior of  $P_t$ , which should decrease continuously with increasing pedogenesis [Walker and Syers, 1976]. Along the climosequence in this study, however,  $P_t$  decreased initially and then increased with decreasing aridity, with the minimum concentrations at an aridity of approximately 0.70 (Figures 2a, 4a, and 5a).

We do not consider variation in parent material to be a major driver of the pattern in total P concentrations across the climosequence. In a transect of the magnitude of that studied here, there will inevitably be some variation in parent material and, therefore, in its P content. Although we do not have detailed information on parent material, soils across the entire 3700 km transect were mostly derived from loess and were of similar elemental composition [Lei et al., 1990; Shi et al., 1990]. Moreover, data from China's second national soil survey [National Soil Survey Office, 1998] shows that  $P_t$  concentrations in C horizons (i.e., horizons unaffected by carbonate leaching) of Haplic Calcisols, Calcic Cambisols, and Calcic Kastanozems in northern China (from three typical soil profiles) were relatively similar: 590–689 mg P kg<sup>-1</sup>, 480–630 mg P kg<sup>-1</sup>, and 550–790 mg P kg<sup>-1</sup>, respectively. Collectively, these results suggest that parent material is well-constrained given the spatial extent of the transect.

Instead, we interpret the pattern of  $P_t$  along the climosequence as reflecting our focus on the surface 10 cm of soil. Surface soil should reflect patterns of P transformations during pedogenesis, as shown along chronosequences [Richardson et al., 2004; Turner et al., 2007; Izquierdo et al., 2013]. However, in humid sites along our climosequence, greater plant productivity [Wang et al., 2014] will concentrate P at the surface via litter returns, counteracting the depletion of  $P_t$  from the surface by leaching [Porder and Chadwick, 2009]. Thus, in drier sites (aridity > 0.7),  $P_o$  concentrations are small due to water limitation of plant growth [Wang et al., 2014] and P occurs mainly as  $P_{Ca}$ , resulting in decline of  $P_t$  along with  $P_{Ca}$  as aridity declines. In contrast,  $P_{Ca}$  is weathered and leached at wetter sites, but P is concentrated at the soil surface as  $P_o$  and occluded P, leading to an increase in  $P_t$  with decreasing aridity (Figure 5a). This not only offers an explanation for the pattern of  $P_t$  observed here along the climosequence but also suggests a potential shift in the P cycle from geochemically dominated to biologically dominated. This shift occurs at an aridity value of 0.7—the approximate point at which the ecosystem shifts from arid to semiarid [United Nations Environment Programme, 1992].

The pattern of nonoccluded  $P_i$  along the climosequence also contrasts with results from chronosequence studies, in which labile P increased continuously in the early stages of soil development [Walker and Syers, 1976; Selmants and Hart, 2010; Chen et al., 2015]. In drier sites, the decline of nonoccluded  $P_i$  along the climosequence in this study might reflect decreasing concentrations of  $P_{Ca}$ , which exert a strong control on P availability in the upper horizons of calcareous soils [Ippolito et al., 2010; Emadi et al., 2012]. In addition, the dominant vegetation types in our drier sites are desert shrub and desert steppe, which typically support little aboveground biomass [Pei et al., 2008]. Delgado-Baquerizo et al. [2013] stated that enhanced geological processes (i.e., wind erosion and photodegradation) due to low vegetation coverage in the most arid sites can promote the release of P from primary minerals, leading to a declining trend of labile P with decreasing aridity. In wetter sites, however, the increased nonoccluded  $P_i$  might reflect increasing  $P_o$  mineralization, because both  $P_o$  and biological activity (i.e., ANPP and MBC) increased along the climosequence (Figure 5a) [Wang et al., 2014]. Schlesinger [1991] observed faster P cycling through  $P_o$  mineralization than through rock weathering in tropical ecosystems and indicated that  $P_o$  recycling is essential to the availability of soil P. Overall, nonoccluded  $P_i$  appears to decline initially in parallel with the decline in  $P_{Ca}$  in drier sites and then increase in parallel with the increase in  $P_o$  in wetter sites, suggesting a gradual transition of P cycling from geochemical to biological processes with soil genesis of the surface soil in these arid and semiarid ecosystems.

The transition of abiotic to biotic control of P cycling is consistent with the results of Delgado-Baquerizo et al. [2013] across an aridity gradient in drylands at global scale. They stated that a difference in the response to aridity of the P cycle compared with that of C and N leads to the decoupling of C, N, and P cycles (manifested as decreases of C:P and N:P) with increasing aridity. However, Wardle [2013] commented that there was no “decoupling” of nutrient cycles and that the decreases of C:P and N:P with increasing aridity appear to operate in the opposite direction to pedogenesis. Our results reconcile this issue by providing evidence for a shift in pedogenic weathering status across the aridity gradient. Specifically, the decoupling of nutrient cycles appears to simply reflect the influence of climate on pedogenesis. Arid conditions slow the rate of weathering, yielding pedogenically young soils with low C:P and N:P ratios (i.e., the decoupling of nutrient cycles) [Walker and Syers, 1976; Crews et al., 1995; Turner and Laliberté, 2015]. The increasing C:P and N:P ratios along the climosequence in this study agree with the results of long-term chronosequence studies, in which P becomes increasingly limiting compared to C and N due to the accumulation of C and N in SOM and the increasing loss of P through leaching with pedogenesis [Walker and Syers, 1976; Crews et al., 1995; Selmants and Hart, 2010; Chen et al., 2015; Turner and Laliberté, 2015]. Here we find a shift of pedogenic weathering status across the aridity gradient from dry to wet, associated with a potential switch in the dominant P turnover pathway from  $P_i$  to  $P_o$  along the climosequence. Should the climate become drier in these arid and semiarid grasslands [Gao and Giorgi, 2008; Feng and Fu, 2013], shifting a site back towards an aridity < 0.7, the dominant control of P cycling would shift to geochemical processes and the P cycle may become decoupled from the C and N cycles [Delgado-Baquerizo et al., 2013; Wardle, 2013]. These results therefore provide evidence for the importance of pedogenic process in regulating the biogeochemical cycling of P and its interaction with C and N cycling in drylands [Delgado-Baquerizo et al., 2013; Wardle, 2013] and have significant implications for predictive models of biogeochemical cycling of nutrients in drylands under global change scenarios.

## 5. Conclusion

The general decline in  $P_{Ca}$  and increases in  $P_o$  and occluded P in soils along this dryland climosequence are consistent with the predictions of the Walker and Syers [1976] model of soil P transformations during pedogenesis. These results indicate a progressive switch from geochemical to biological control of the P cycle as aridity declines across an aridity value of about 0.7. The changes in P composition occur concurrently with increasing C: $P_o$  and N: $P_o$  ratios, indicating declining abundance of P relative to N along the climosequence. Overall, these results suggest that the Walker and Syers [1976] model can be applied to climosequences in arid and semiarid ecosystems.

## References

- Agbenin, J., and H. Tiessen (1995), Phosphorus forms in particle-size fractions of a toposequence from northeast Brazil, *Soil Sci. Soc. Am. J.*, 59(6), 1687–1693.
- Arora, V. K. (2002), The use of the aridity index to assess climate change effect on annual runoff, *J. Hydrol.*, 265(1), 164–177.

### Acknowledgments

This study was supported by the National Natural Science Foundation of China (41171241 and 41201290) and the Strategic Priority Research Program of the Chinese Academy of Sciences (XDB15010400). XT Lü was supported by Youth Innovation Promotion Association, CAS (2014174). We wish to thank Xingguo Han, Xiaobo Wang, and all the members of Shenyang sampling campaign teams from Institute of Applied Ecology, Chinese Academy of Sciences, for their assistance during field sampling. We thank the anonymous reviewers for insightful comments that improved the manuscript. Data on variations of soil phosphorus fractions across the aridity gradient are provided as online supporting information (see Figure S1). The authors declare no conflict of interest. Correspondence and requests for materials could be addressed to Lijun Chen (ljchenchina@hotmail.com; ljchen@iae.ac.cn).

- Aspila, K., H. Agemian, and A. Chau (1976), A semi-automated method for the determination of inorganic, organic and total phosphate in sediments, *Analyst*, *101*(1200), 187–197.
- Celi, L., S. Lamacchia, F. Marsan, and E. Barberis (1999), Interaction of inositol hexaphosphate on clays: Adsorption and charging phenomena, *Soil Sci.*, *164*, 574–585.
- Chen, C., E. Hou, L. Condron, G. Bacon, M. Esfandbod, J. Olley, and B. Turner (2015), Soil phosphorus fractionation and nutrient dynamics along the Cooloola coastal dune chronosequence, southern Queensland, Australia, *Geoderma*, doi:10.1016/j.geoderma.2015.1004.1027.
- Craine, J. M., C. Morrow, and W. D. Stock (2008), Nutrient concentration ratios and co-limitation in South African grasslands, *New Phytol.*, *179*(3), 829–836.
- Crews, T. E., K. Kitayama, J. H. Fownes, R. H. Riley, D. A. Herbert, D. Mueller-Dombois, and P. M. Vitousek (1995), Changes in soil phosphorus fractions and ecosystem dynamics across a long chronosequence in Hawaii, *Ecology*, *76*(5), 1407–1424.
- Cross, A. F., and W. H. Schlesinger (1995), A literature review and evaluation of the Hedley fractionation: Applications to the biogeochemical cycle of soil phosphorus in natural ecosystems, *Geoderma*, *64*(3), 197–214.
- Cross, A. F., and W. H. Schlesinger (2001), Biological and geochemical controls on phosphorus fractions in semiarid soils, *Biogeochemistry*, *52*(2), 155–172.
- Delgado-Baquerizo, M., F. T. Maestre, A. Gallardo, M. A. Bowker, M. D. Wallenstein, J. L. Quero, V. Ochoa, B. Gozalo, M. García-Gómez, and S. Soliveres (2013), Decoupling of soil nutrient cycles as a function of aridity in global drylands, *Nature*, *502*(7473), 672–676.
- Emadi, M., M. Baghernejad, M. A. Bahmanyar, and A. Morovvat (2012), Changes in soil inorganic phosphorous pools along a precipitation gradient in northern Iran, *Int. J. Forest. Soil Erosi.*, *2*(3), 143–147.
- Food and Agriculture Organization (1993), Global and national soils and terrain digital databases (SOTER): Procedures manual, in *World Soil Resources Reports*, Food and Agriculture Organization of the United Nations, Rome, Italy.
- Feng, S., and Q. Fu (2013), Expansion of global drylands under a warming climate, *Atmos. Chem. Phys.*, *13*(10), 081–010.
- Feng, Z.-D., C. An, and H. Wang (2006), Holocene climatic and environmental changes in the arid and semi-arid areas of China: A review, *Holocene*, *16*(1), 119–130.
- Gao, X., and F. Giorgi (2008), Increased aridity in the Mediterranean region under greenhouse gas forcing estimated from high resolution simulations with a regional climate model, *Global Planet. Change*, *62*(3), 195–209.
- Hance, R., and G. Anderson (1962), A comparative study of methods of estimating soil organic phosphate, *J. Soil Sci.*, *13*(2), 225–230.
- Ippolito, J., S. Blecker, C. Freeman, R. McCulley, J. Blair, and E. Kelly (2010), Phosphorus biogeochemistry across a precipitation gradient in grasslands of central North America, *J. Arid Environ.*, *74*(8), 954–961.
- Irwin-Williams, C., and C. V. Haynes (1970), Climatic change and early population dynamics in the southwestern United States, *Quaternary Res.*, *1*(1), 59–71.
- Izquierdo, J. E., B. Z. Houlton, and T. L. V. Huysen (2013), Evidence for progressive phosphorus limitation over long-term ecosystem development: Examination of a biogeochemical paradigm, *Plant Soil*, *367*(1–2), 135–147.
- Khormali, F., and M. Kehl (2011), Micromorphology and development of loess-derived surface and buried soils along a precipitation gradient in Northern Iran, *Quatern. Int.*, *234*(1), 109–123.
- Lajtha, K., and W. H. Schlesinger (1988), The biogeochemistry of phosphorus cycling and phosphorus availability along a desert soil chronosequence, *Ecology*, *69*(1), 24–39.
- Lei, W., R. Huang, and J. Li (1990), Desert soils, in *Soils of China*, edited by C. Li and O. Sun, pp. 173–190, Science Press, Beijing, China.
- Liangwu, L., and M. Angjiang (2001), Radiocarbon ages of soils in China, *Acta Pedo. Sinica.*, *38*(4), 513–520.
- Luo, W. (2015), Zonal differentiation of elements in soil-plant system across Northern China's grassland, PhD dissertation, pp. 61–93, Univ. of Chinese Academy of Sciences, Shenyang.
- Luo, W. T., et al. (2015), Plant nutrients do not covary with soil nutrients under changing climatic conditions, *Global Biogeochem. Cycles*, *29*, 1298–1308, doi:10.1002/2015GB005089.
- Luo, W., F. A. Dijkstra, E. Bai, J. Feng, X.-T. Lü, C. Wang, H. Wu, M.-H. Li, X. Han, and Y. Jiang (2016), A threshold reveals decoupled relationship of sulfur with carbon and nitrogen in soils across arid and semi-arid grasslands in northern China, *Biogeochemistry*, *127*(1), 141–153.
- Mackenzie, F. T., L. M. Ver, and A. Lerman (2002), Century-scale nitrogen and phosphorus controls of the carbon cycle, *Chem. Geol.*, *190*(1), 13–32.
- McGroddy, M. E., W. L. Silver, R. C. Oliveira, W. Z. Mello, and M. Keller (2008), Retention of phosphorus in highly weathered soils under a lowland Amazonian forest ecosystem, *J. Geophys. Res.*, *113*, G04012, doi:10.1029/2008JG000756.
- National Soil Survey Office (1998), *National Soil Survey Office, Soil of China*, China Agriculture Press, Beijing.
- Okin, G. S., N. Mahowald, O. A. Chadwick, and P. Artaxo (2004), Impact of desert dust on the biogeochemistry of phosphorus in terrestrial ecosystems, *Global Biogeochem. Cycles*, *18*, GB2005, doi:10.1029/2003GB002145.
- Pei, S. F., H. Fu, and C. G. Wan (2008), Changes in soil properties and vegetation following enclosure and grazing in degraded Alxa desert steppe of Inner Mongolia, China, *Agric. Ecosyst. Environ.*, *124*(1–2), 33–39.
- Porder, S., and O. A. Chadwick (2009), Climate and soil-age constraints on nutrient uplift and retention by plants, *Ecology*, *90*(3), 623–636.
- Post, W. M., J. Pastor, P. J. Zinke, and A. G. Stangenberger (1985), Global patterns of soil nitrogen storage, *Nature*, *317*(6038), 613–616.
- Quénard, L., A. Samouëlian, B. Laroche, and S. Cornu (2011), Lessivage as a major process of soil formation: A revisit of existing data, *Geoderma*, *167*, 135–147.
- Richardson, S. J., D. A. Peltzer, R. B. Allen, M. S. McGlone, and R. L. Parfitt (2004), Rapid development of phosphorus limitation in temperate rainforest along the Franz Josef soil chronosequence, *Oecologia*, *139*(2), 267–276.
- Roberts, T., J. Stewart, and J. Bettany (1985), The influence of topography on the distribution of organic and inorganic soil phosphorus across a narrow environmental gradient, *Can. J. Soil Sci.*, *65*(4), 651–665.
- Schlesinger, W. (1991), *Biogeochemistry: An Analysis of Global Change*, Academic Press, San Diego, Calif.
- Selmants, P. C., and S. C. Hart (2010), Phosphorus and soil development: Does the Walker and Syers model apply to semiarid ecosystems?, *Ecology*, *91*(2), 474–484.
- Shi, Y., W. Cai, and Y. Gao (1990), Castanozems, brown pedocals and sierozems, in *Soils of China*, edited by C. Li and O. Sun, pp. 154–167, Science Press, Beijing, China.
- Syers, J. K., and T. W. Walker (1969a), Phosphorus transformations in a chronosequence of soils development on wind-blown sand in New Zealand: II. Inorganic phosphorus, *J. Soil Sci.*, *20*(2), 318–324.
- Syers, J. K., and T. W. Walker (1969b), Phosphorus transformations in a chronosequence of soils development on wind-blown sand in New Zealand: I. Total and organic phosphorus, *J. Soil Sci.*, *20*(1), 57–64.
- Tiessen, H., and J. Moir (1993), Characterization of available P by sequential extraction, in *Soil Sampling and Methods of Analysis*, edited by M. R. Carter, pp. 5–229, Lewis Publishers, Ann Arbor.

- Tiessen, H., J. Stewart, and C. Cole (1984), Pathways of phosphorus transformations in soils of differing pedogenesis, *Soil Sci. Soc. Am. J.*, *48*(4), 853–858.
- Turner, B. L., and E. Laliberté (2015), Soil development and nutrient availability along a 2 million-year coastal dune chronosequence under species-rich Mediterranean shrubland in Southwestern Australia, *Ecosystems*, *18*(2), 1–23.
- Turner, B. L., and L. M. Condrón (2013), Pedogenesis, nutrient dynamics, and ecosystem development: The legacy of TW Walker and JK Syers, *Plant Soil*, *367*(1–2), 1–10.
- Turner, B. L., M. J. Papházy, P. M. Haygarth, and I. D. McKelvie (2002), Inositol phosphates in the environment, *Philos. Trans. R. Soc.*, *357*(1420), 449–469.
- Turner, B. L., L. M. Condrón, S. J. Richardson, D. A. Peltzer, and V. J. Allison (2007), Soil organic phosphorus transformations during pedogenesis, *Ecosystems*, *10*(7), 1166–1181.
- United Nations Environment Programme (1992), *World Atlas of Desertification Edited*, Edward Arnold, Seven Oaks, Nairobi, Kenya.
- Vitousek, P. M., and H. Farrington (1997), Nutrient limitation and soil development: Experimental test of a biogeochemical theory, *Biogeochemistry*, *37*(1), 63–75.
- Vitousek, P. M., S. Porder, B. Z. Houlton, and O. A. Chadwick (2010), Terrestrial phosphorus limitation: Mechanisms, implications, and nitrogen-phosphorus interactions, *Ecol. Appl.*, *20*(1), 5–15.
- Walker, T. (1965), The significance of phosphorus in pedogenesis, in *Experimental Pedology*, edited by E. Hallsforth, pp. 295–315, Butterworths, London, U. K.
- Walker, T., and A. R. Adams (1958), Studies on soil organic matter: I. Influence of phosphorus content of parent materials on accumulations of carbon, nitrogen, sulfur, and organic phosphorus in grassland soils, *Soil Sci.*, *85*(6), 307–318.
- Walker, T., and J. Syers (1976), The fate of phosphorus during pedogenesis, *Geoderma*, *15*(1), 1–19.
- Wang, C., et al. (2014), Aridity threshold in controlling ecosystem nitrogen cycling in arid and semi-arid grasslands, *Nat. Commun.*, *5*, doi:10.1038/ncomms5799.
- Wang, X. G., S. A. Sistla, X. B. Wang, X. T. Lü, and X. G. Han (2016), Carbon and nitrogen contents in particle-size fractions of topsoil along a 3000 km aridity gradient in northern China, *Biogeosciences*, *13*, 3635–3646.
- Wardle, D. A. (2013), Ecology: Drivers of decoupling in drylands, *Nature*, *502*(7473), 628–629.
- Williams, J., J. K. Syers, and T. Walker (1967), Fractionation of soil inorganic phosphate by a modification of Chang and Jackson's procedure, *Soil Sci. Soc. Am. J.*, *31*(6), 736–739.
- Williams, J., J. Syers, T. Walker, and R. Rex (1970), A comparison of methods for the determination of soil organic phosphorus, *Soil Sci.*, *110*(1), 13–18.
- Yang, X., and W. Post (2011), Phosphorus transformations as a function of pedogenesis: A synthesis of soil phosphorus data using Hedley fractionation method, *Biogeosciences*, *8*, 2907–2916.
- Zheng, Z.-M., G.-R. Yu, Y.-L. Fu, Y.-S. Wang, X.-M. Sun, and Y.-H. Wang (2009), Temperature sensitivity of soil respiration is affected by prevailing climatic conditions and soil organic carbon content: A trans-China based case study, *Soil Biol. Biochem.*, *41*(7), 1531–1540.
- Zhou, G., Y. Wang, and S. Wang (2002), Responses of grassland ecosystems to precipitation and land use along the Northeast China Transect, *J. Veg. Sci.*, *13*(3), 361–368.